Transcranial contrast-enhanced ultrasound in the rat brain reveals substantial hyperperfusion acutely post-stroke

Dino Premilovac[1], Sarah J. Blackwood[2], Ciaran J. Ramsay[1], Michelle A. Keske[3], David W. Howells[1] and Brad A. Sutherland[1]

[1] School of Medicine, College of Health and Medicine, University of Tasmania, Hobart, Tasmania, Australia

[2] Åstrand Laboratory of Work Physiology, Swedish School of Sport and Health Sciences, GIH, Stockholm, Sweden

[3] Institute for Physical Activity and Nutrition (IPAN), School of Exercise and Nutrition Sciences, Deakin University, Geelong, Victoria, Australia.

Running title: Cerebral perfusion with CEU during stroke

Corresponding Author:

Brad A. Sutherland (PhD)

School of Medicine, College of Health and Medicine, University of Tasmania

Hobart, TAS 7000, Australia

P: +61 3 6226 7634

brad.sutherland@utas.edu.au

Abstract

Direct and real-time assessment of cerebral hemodynamics is key to improving our understanding of cerebral blood flow regulation in health and disease states such as stroke. While a number of sophisticated imaging platforms enable assessment of cerebral perfusion, most are limited either spatially or temporally. Here, we applied transcranial contrast enhanced ultrasound (CEU) to measure cerebral perfusion in real-time through the intact rat skull before, during and after ischemic stroke, induced by intraluminal filament middle cerebral artery occlusion (MCAO). We demonstrate expected decreases in cortical and striatal blood volume, flow velocity and perfusion during MCAO. After filament retraction, blood volume and perfusion increased two-fold above baseline, indicative of acute hyperperfusion. Adjacent brain regions to the ischemic area and the contralateral hemisphere had increased blood volume during MCAO. We assessed our data using wavelet analysis to demonstrate striking vasomotion changes in the ischemic and contralateral cortices during MCAO and reperfusion. In conclusion, we demonstrate the application of CEU for real-time assessment of cerebral hemodynamics and show that the ischemic regions exhibit striking hyperemia post-MCAO. Whether this post-stoke hyperperfusion is sustained long-term and contributes to stroke severity is not known.

Keywords

Ischemic stroke, contrast-enhanced ultrasound, cerebral blood flow, middle cerebral artery occlusion, rat

Introduction

Ischemic stroke is characterized by an abrupt cessation of blood flow to a region of the brain leading to irreversible neuronal damage within the ischemic core. This central infarct core is surrounded by an area of diminished blood supply called the penumbra which has enough residual flow to allow neurons to survive until restoration of flow has occurred.[1] The importance of blood flow changes, in particular reperfusion, to stroke outcomes has been observed both in human studies[2] and animal models.[3, 4] Recanalization of the occluded vessel by either pharmacological or mechanical means is currently the main modality for the treatment of ischemic stroke patients. Therefore, improving our understanding of cerebral blood flow kinetics and how these change during ischemia and reperfusion will provide valuable insight into the pathophysiology of stroke and provide a better understanding of how to improve treatment of stroke. This is particularly important in the era of endovascular thrombectomy where reperfusion of the cerebral vasculature post-stroke is rapid[5-7].

Multiple techniques have been developed to assess blood flow changes in the human brain including magnetic resonance imaging (MRI; arterial spin labelling), CT perfusion, cerebral angiography, positron emission topography ([^{15}O]-water), and transcranial Doppler.[8-11] However, these techniques are limited by their spatial resolution and sampling frequency (the amount of time taken for a single measure). The use of animal models of stroke allows continuous measurement of blood flow with greater spatial and temporal resolution than the techniques used in humans. Techniques such as Laser Doppler Flowmetry (LDF), Laser Speckle Contrast Imaging, ^{14}C-iodoantipyrine autoradiography and hydrogen clearance[12-15] but also optical techniques such as optical

coherence tomography, photoacoustic microscopy, optical imaging spectroscopy and two-photon microscopy[16] have been used in animal studies. These techniques require invasive surgical (i.e. thinning or removal of part of the skull) or terminal procedures to acquire information about blood flow. This makes their value in the post-stroke setting limited. Therefore, developing methods that allow high spatial and temporal assessment of blood flow changes in real-time during ischemia and reperfusion will improve our understanding of blood flow kinetics during and after stroke.

Contrast enhanced ultrasound (CEU) utilizes an intravenous infusion of a contrast agent, typically albumin or phospholipid microbubbles (filled with perfluorocarbon gas) to enable direct assessment of the vasculature using ultrasound. These microbubbles are similar in both size and rheology to red blood cells[17, 18], and importantly they remain exclusively intravascular making them an excellent vascular tracer. When exposed to ultrasound, microbubbles oscillate in size generating acoustic reflections that can be detected by the ultrasound transducer. A high intensity burst of ultrasound can also be used to destroy microbubbles in the vasculature to enable the quantification of microbubble (and hence blood) refill kinetics back through the underlying vasculature. CEU has previously been used to interrogate and quantify blood flow changes in peripheral tissues such as the heart, adipose tissue, kidney and skeletal muscle.[17, 19-22] CEU has also been used to quantify brain perfusion in dogs and humans typically with part of the skull removed by craniotomy.[23, 24] Two studies by the same group have applied CEU to assess brain perfusion in acute stroke patients with the skull intact by placing the ultrasound transducer on the temple (where the skull is relatively thin) to assess the brain regions immediately behind the temple.[25, 26] However, the routine use of CEU for stroke imaging has not been

adopted clinically due to problems with skull attenuation of the ultrasound signal preventing imaging of the entire brain and the variability of CEU measurement inherent when using bolus microbubble injections to accurately assess blood volume and velocity. A more recent study in rats showed that functional ultrasound (fUS; 500Hz) combined with intravenous microbubble bolus injections could be used to detect small changes in cerebral blood flow in a rat model of functional hyperemia without thinning the skull,[27] suggesting that the rat model could be an excellent model for using CEU non-invasively to determine blood flow kinetics across the entire brain. Here, we highlight the ability to image cerebral blood flow with transcranial CEU in real-time and non-invasively in rats before, during and after ischemic stroke using steady-state microbubble infusion to measure changes in cerebral blood flow kinetics.

Materials and Methods

Animals

All animal procedures conformed with current NIH guidelines, were performed in accordance with the Australian Code of Practice for the Care and Use of Animals for Scientific Purposes–2013 (8th Edition) and approved by the University of Tasmania Animal Ethics Committee. All rats were supplied by the Cambridge Farm Facility, University of Tasmania, housed in standard rat caging in a 12h light:dark cycle and had *ad libitum* access to food and water. Sixteen adult, male Sprague-Dawley rats (370-420g) underwent surgical procedures for an intravenous cannulation and induction of middle cerebral artery occlusion (MCAO) as described below. All data and underlying materials are available upon request and all data are reported in accordance to the ARRIVE guidelines.

Anesthesia and cannulation

Rats were anesthetized with either a 1.2g/kg i.p. injection of urethane (Sigma Aldrich, MO, USA) and provided with a 0.1g/kg top-up dose if required, or 5% isoflurane carried in 95% oxygen and maintained with 1.5-2% isoflurane carried in 98-98.5% oxygen. Respiration rate and response to tail and foot pinch were monitored throughout the procedure to assess depth of anesthesia. Body temperature was monitored with a rectal probe and maintained at 37.0±1.0°C with a heated mat. After anesthesia, neck microsurgery was performed to cannulate a branch of the left external jugular vein. A polyethylene cannula (PE40; Microtube Extrusions, North Rocks, NSW, Australia) filled

with heparinized saline was implanted into the jugular vein and secured with surgical silk to enable intravenous infusion of phospholipid microbubbles for CEU imaging.

Middle cerebral artery occlusion

A similar procedure to Sutherland and Buchan[4] was followed. In brief, rats had their right external carotid, common carotid and internal carotid arteries carefully exposed. The external carotid artery was permanently cauterized with a bipolar cauterizer (ForceFX Valleylab, Medtronic, Dublin, Ireland) and cut to form a stump. The common and internal carotid arteries were temporarily ligated with either 3-0 sutures or a hemostatic clip. Following common carotid artery occlusion (CCAO) we assessed changes in cerebral blood flow using CEU as outlined below. After CCAO imaging, a small arteriotomy was made in the external carotid artery stump and a silicon-tipped filament (404156PK10, Doccol Corporation, USA) was inserted into the external carotid artery. The filament was advanced up the internal carotid artery until resistance was felt indicating the filament was lodged in the origin of the middle cerebral artery. Following middle cerebral artery occlusion (MCAO), we assessed cerebral blood flow using CEU as outlined below. The filament remained in place for 45, 60 or 90 minutes after which it was withdrawn to produce middle cerebral artery recanalization. At this time, common carotid artery ligation was released to allow full recanalization of the arterial system. After CEU imaging was completed, rats were quickly euthanized with a lethal intracardiac injection of pentobarbitone (200mg/kg).

Contrast enhanced ultrasound setup

To enable vascular imaging of the brain, the fur on the head was first removed using an electric shaver. Following application of ultrasonic gel (Aquasonic, Parker Laboratories Inc, Fairfield, NJ, USA) to the head, a linear array transducer (L12-5) was positioned over either the left or right side of the head in the longitudinal plane (~15° from the midline) to enable visualization of an entire brain hemisphere in the sagittal orientation as shown in figure 1a. Three landmarks - the eye, ear canal and large artery at the rear of the skull (see figures 1a and 1b) were used to position the transducer in the same plane/position when moving the transducer from one side of the head to the other and between different animals. The outline of the brain can be visualized clearly on the tissue ultrasound image when compared to the sagittal section of a dissected rat brain (figure 1b). The sagittal orientation was chosen to enable CEU detection without skull thinning, as the ultrasound signal was attenuated beneath the thick bone that covers the midline of the rat skull when imaged in the coronal plane (data not shown). The transducer was interfaced with an iU22 ultrasound machine (Philips Medical Systems, Australia) and real-time (15.2Hz), low mechanical index (0.24) imaging was performed during a constant infusion of phospholipid microbubbles (Definity®, Lantheus Medical Imaging, Australia). Prior to their infusion, a stock solution of microbubbles was reconstituted using a vial mixer and diluted in sterile heparinized saline (0.8ml into 5ml total). The ultrasound gain settings (94%), compression (C=39), depth (2 cm) and focus were kept constant for all experiments. The rate of intravenous microbubble infusion (50µl/min) required to obtain a strong, but not saturated CEU signal from the brain vasculature was optimized in preliminary experiments (supplementary figure 1). An infusion rate of 50µl/min was also chosen to

limit total blood volume expansion due to microbubble infusion across the length of the experiment.

Transcranial contrast enhanced ultrasound imaging

As outlined in the protocol (figure 1c), transcranial CEU imaging of left and right hemispheres was performed at baseline, following CCAO, MCAO and reperfusion. In all instances, the right hemisphere (the side undergoing MCAO, termed ipsilateral) was imaged first, followed immediately by the unaffected, left hemisphere (contralateral). A 9-minute infusion of microbubbles was used to ensure steady-state arterial concentration of microbubbles prior to quantification of vascular refill kinetics. High mechanical index (1.20) ultrasound pulses can be used to destroy microbubbles in the vasculature under the ultrasound probe (see figure 1d, supplementary figure 2 and supplementary videos 1-4). Preliminary experiments showed that a burst of four pulses was needed to destroy microbubbles to the greatest extent (supplementary figure 2), which was used for all subsequent experiments quantifying vascular refill kinetics. The first frame captured following this high intensity burst of ultrasound was used to subtract the contribution of the background tissue signal from the vascular, microbubble signal. The refill of microbubbles through the cerebral vasculature was recorded and quantified over the subsequent 60 seconds (figure 1d). This sequence was repeated three times for each of the experimental time-points outlined in figure 1c and the three measures were averaged to obtain one refill curve for each time-point (example refill curves are shown in figures 1d, 3 and 4 and supplementary figures 3, 6 and 7). The resulting acoustic intensity curves were plotted versus time as shown in figure 1d and the data were fitted to the function:

$$y = a\,(1 - e^{(-\beta t)})$$

Where *y* is acoustic intensity at time *t*, *a* is plateau acoustic intensity (blood volume) and β is the slope of the curve (flow velocity) as previously described.[28] Vascular perfusion was calculated as the product of a x β. We have used this analysis previously to determine changes in blood volume, flow velocity and vascular perfusion in peripheral tissues such as skeletal muscle.[21, 22] Supplementary figure 3 shows that overall acoustic intensity was not altered during the sequence of three microbubble destruction and refill curves, 60 seconds was sufficient for complete reperfusion of microbubbles through the cerebrovasculature and that baseline acoustic intensity or oscillations were not altered following repeated microbubble destruction.

The acoustic intensity signal plateau during microbubble refill following destructive high ultrasound pulses is an indicator of blood volume (see figure 1d). From these images, blood volume maps for each of the four timepoints (baseline, CCAO, MCAO and reperfusion) were generated by calculating the average acoustic intensity at 60 seconds following microbubble destruction throughout the brain (figure 2a). As well as quantification of vascular volume, flow velocity and perfusion, the same destruction-refill curves can be used to visually track microbubble transit through the vascular tree after ultrasonic destruction. This mode of CEU imaging, termed microvascular imaging (MVI; see figures 1b, supplementary figures 4 and 5, and supplementary video 5) was applied post-hoc to the 60 second destruction-refill data obtained at each of the four time-points outlined in the protocol above. While MVI does not provide a quantitative measure of cerebral blood flow, it is a powerful tool that can be used to quickly identify regions of the brain where perfusion has been altered.

Vasomotion analysis

Prior to assessment of cerebral hemodynamics, a 9-minute infusion of microbubbles (50µ/min) was used to ensure steady state arterial concentration (see supplementary figure 3). This 9-minute infusion was recorded at 15.2Hz and the acoustic intensity for the cortical region (see figure 3 for region of interest) was exported for processing using MATLAB (MathWorks, Natick, MA, USA). Vasomotion analysis was performed as recently published.[29] Briefly, MATLAB was used to perform wavelet transformation using the well-established 2:1 cmor morlet wavlet.[30] Before wavelet transformation, the average value of the data set was determined and then subtracted from each data point. For the spectral analysis, the wavelet transformation technique was chosen because it allows a more precise determination of the lower frequency components of a signal.[31] The area under the curve (AUC) for the total frequency range for each time-point (baseline, CCAO, MCAO and reperfusion) was averaged to give an experimental output for both the ipsilateral and contralateral cortices. In addition, we performed a frequency analysis to assess the contribution of cardiac (4-10 Hz) and respiratory (0.15-4.0 Hz) rate on cortical vasomotion as previously described.[29]

Histology

To determine whether the drop in cerebral blood flow observed in the cortex and striatum led to histological changes in the brain, we conducted an experiment where a rat underwent MCAO with CEU imaging to confirm deficits in vascular perfusion. After 6 hours of MCAO, euthanasia was induced by a lethal intraperitoneal injection of pentobarbitone (200mg/kg). The brain was extracted following decapitation and sliced into 2mm sections sagitally using a brain matrix (Alto, Cell Point Scientific, Gaitherburg, MD, USA). Brain sections were incubated in 2% 2,3-triphenyltetrazolium chloride (TTC,

Sigma) in PBS for 30 minutes at 37°C and photographed. TTC clearly delineates between viable tissue (red/pink stain) and infarcted tissue (white).

Statistical analysis

All ultrasound data were exported from the iU22 ultrasound machine and specific regions of interest were analysed using QLAB Advanced Quantification Software (Philips). Images from CEU and MVI files were processed in Image J (U. S. National Institutes of Health, Bethesda, Maryland, USA) to produce 8-bit images prior to application of heat mapping (figure 2 and supplementary figures 4 and 5). All images were treated in the same manner and any adjustments were applied to all images. Blood flow kinetics were analysed and quantified across four specific regions representing (i) the cortical region, (ii) the striatal region, (iii) the posterior sub-cortical region and (iv) the whole hemisphere. Data are presented as means ± SD unless otherwise specified and statistical differences were determined using Sigma Plot 11 (Systat Software Inc, 2011, San Diego, CA, USA). Comparisons between ipsilateral and contralateral hemispheres at different time-points were performed by two-way repeated measures ANOVA. When a significant difference of $p<0.05$ was detected, Student-Newman-Keuls post-hoc was used to assess differences. All animals were included in analyses with no animals excluded for any reason.

Results

Mapping cererbral hemodynamics using CEU during MCAO and reperfusion

First, we wished to assess vascular perfusion changes in the brain during MCAO and reperfusion using CEU. We used a destructive ultrasound pulse to clear the microbubbles from the vasculature, followed by assessment of microbubble reappearance through the vasculature across 60 seconds (supplementary videos 1-4). This enabled us to spatially map blood volume in the brain at baseline, during MCAO and reperfusion (figure 2a). Our results demonstrated that MCAO substantially reduced blood volume primarily in the cortex but also in the striatum. Following retraction of the filament and recanalization of both the middle cerebral and common carotid arteries, a considerable hyperperfusion was apparent, particularly in the cortex. These results were consistent with the MVI function where microbubbles can be tracked in real-time throughout the cerebral vasculature (supplementary figures 4 and 5 and supplementary video 5). Relative to baseline, MCAO reduced the extent of perfusion in the ipsilateral hemisphere (figure 2a and supplementary figure 4) while minimal change was observed in the contralateral hemisphere (supplementary figure 5). Upon reperfusion, blood flow appeared to be dramatically elevated compared to both the contralateral side and the ipsilateral baseline (figure 2a and supplementary figures 4 and 5).

Next, we wanted to compare the identity of brain regions affected by MCAO using CEU in the sagittal plane with histological damage. Initially, we performed CEU imaging following MCAO and compared vascular perfusion to baseline levels. Figure 2b shows a substantial reduction in vascular perfusion in both cortical and striatal brain regions. TTC staining of the same brain 6 hours following permanent MCAO revealed injury to both

striatal and cortical regions that were easily identified using CEU (figure 2b). We next quantified changes in vascular perfusion in these specific brain regions using transcranial CEU before, during and after transient stroke.

Real-time assessment of cortical-specific hemodynamics before, during and after stroke

At baseline, CCAO, MCAO and reperfusion, we quantified blood flow kinetics across both the ipsilateral and contralateral hemispheres using CEU destruction-refill analysis as illustrated in figure 1d. We first assessed region specific alterations in hemodynamics by focusing our analysis on the cortex (figure 3a, ROI volume = 176.2 ± 9.9 mm^3) as it is predominantly supplied by the middle cerebral artery (which is occluded with the MCAO model). Compared to the contralateral cortex, the ipsilateral cortex had a modest reduction in blood volume during CCAO (figure 3d; p=0.061) and a striking reduction following MCAO (p=0.002). Intriguingly, we observed a dramatic, more than two-fold increase in blood volume following reperfusion in the ipsilateral cortex relative to both the ipsilateral baseline (p<0.001) and the contralateral cortex at reperfusion (p<0.001). Flow velocity in the ipsilateral cortex was similarly reduced following both CCAO (figure 3e; p=0.009) and MCAO (p<0.001) and increased following reperfusion (p=0.018) relative to the contralateral side. Vascular perfusion within the ipsilateral cortex was reduced during CCAO (figure 3f; p=0.027) and decreased to 18% of the contralateral cortex following MCAO (p<0.001). As above, we observed a dramatic increase in vascular perfusion in the ipsilateral cortex following reperfusion relative to both the ipsilateral baseline (p<0.001) and the contralateral cortex at reperfusion (p<0.001).

Real-time assessment of striatal haemodynamics before, during and after stroke

We then focused our analysis on the primary sub-cortical region that is affected by MCAO, the striatum (figure 4a, ROI volume = 156.9 ± 7.5 mm^3). Overall, there were similar effects in the striatum as the cortex but to a lesser extent. Blood volume within the ipsilateral striatal region (figure 4d) was unchanged during CCAO (p=0.416), was significantly decreased during MCAO (p=0.017) and increased following reperfusion (p<0.001) relative to baseline. There was a reduction in flow velocity in the striatum during both CCAO (figure 4e; p=0.007) and MCAO (p=0.003) whereas reperfusion restored flow velocity to baseline levels. We observed a substantial drop in vascular perfusion during CCAO (figure 4f; p=0.026) and MCAO (p=0.003) with a significant rise in perfusion above baseline during reperfusion (p=0.01). There was no significant change in vascular perfusion in the striatum in the contralateral hemisphere at any time point.

Real-time assessment of hemodynamics in the posterior sub-cortical brain region and the whole hemisphere before, during and after stroke

The posterior sub-cortical region includes areas such as the thalamus and receives its blood supply primarily from the posterior cerebral arteries. In contrast to the cortical- and striatal-specific changes noted above, blood volume, flow velocity and vascular perfusion was not altered in the ipsilateral posterior sub-cortical region at any timepoint relative to baseline (supplementary figure 6). Interestingly, there was a significant increase in blood volume in the contralateral posterior sub-cortical region during CCAO (p=0.015) and MCAO (p=0.017) that returned to baseline levels during reperfusion.

We also quantified hemodynamics throughout the entire ipsilateral and contralateral hemispheres during CCAO, MCAO and reperfusion (supplementary figure 7). Compared to baseline, we found that MCAO reduced blood volume (panel D; p=0.028), flow velocity

(panel E; p=0.002) and vascular perfusion (panel F; p=0.013). Although flow velocity and vascular perfusion were restored to baseline levels at reperfusion, we found that blood volume was markedly increased (p<0.001) within the ipsilateral hemisphere compared to baseline. Intriguingly, we found that blood volume within the contralateral hemisphere tended to be higher than the contralateral baseline at CCAO (panel D; p=0.046), MCAO (p=0.057) and reperfusion (p=0.051).

Assessing cortical vasomotion using CEU before, during and after stroke

A 9-minute infusion of microbubbles was used to ensure steady state concentration prior to assessment of cerebral hemodynamics using destruction-refill kinetics as noted above. Representative 9-minute infusions for one experiment are shown in figure 5 for both the ipsilateral cortex (panel A) and contralateral cortex (panel B). We applied spectral analysis to these data (figure 5; panel C) to assess the extent of overall vasomotion changes at baseline, CCAO, MCAO and reperfusion. While ipsilateral cortical vasomotion was slightly reduced during CCAO (p=0.245 vs baseline) and MCAO (p=0.125 vs baseline), this was not statistically different from baseline. In contrast, vasomotion was increased approximately 2-fold at reperfusion compared to baseline (p<0.001). No statistically different changes were observed in vasomotion in the contralateral cortex at CCAO (p=0.129), MCAO (p=0.125) and reperfusion (p=0.061) compared to the contralateral baseline. While vasomotion in the contralateral cortex was increased at CCAO (p=0.008) and MCAO (p=0.001) compared with the ipsilateral cortex, at reperfusion contralateral vasomotion was far lower than the ipsilateral side at the same time-point (p<0.001).

In addition, using a specified frequency analysis,[29] we also determined the contribution of cardiac and respiratory rate on cortical vasomotion (table 1). Heart rate was the major contributor to total cortical vasomotion (55-63%) with respiration accounting for 27-33% of total cortical vasomotion. During reperfusion, there was a significant increase in the cardiac contribution to vasomotion ($p<0.05$) with a concomitant decrease in the respiratory contribution ($p<0.05$) in the ipsilateral cortex. This suggests that heart rate has a major influence on vasomotion as well the extent of blood flowing through the brain.

Real-time assessment of cortical hemodynamics with different durations of occlusion

Next, we investigated whether the hyperperfusion response observed above after 60 minutes of MCAO also occurs following differing durations of MCAO. We performed additional CEU experiments to compare the extent of reperfusion following 45 minutes, 60 minutes or 90 minutes of MCAO. Figure 6 shows that MCAO reduced cortical vascular perfusion to a similar extent across all three groups. Regardless of the duration of MCAO, there was a substantial hyperperfusion (197-245% of baseline levels) following retraction of the filament. This increase in cortical reperfusion post-MCAO was not significantly different between the three groups.

The cortical vascular perfusion results during MCAO from our CEU work are similar to cortical blood flow changes as measured by the well accepted LDF technique in a historical cohort of rats undergoing the exact same MCAO model (supplementary figure 8).[4] When comparing the two techniques, the reduction in cortical perfusion during 90 minutes MCAO was similar between CEU (figure 6; 28% ± 14% of baseline) and LDF (supplementary figure 8; 23% ± 13% of baseline). However, once blood flow was restored

following filament retraction, cortical vascular perfusion was substantially greater when measured by CEU (246% ± 60% of baseline) compared to LDF (74% ± 22% of baseline). Unfortunately, physical constraints with the experimental setup meant that LDF and CEU measurements could not be conducted on the same animal.

Discussion

The brain is arguably the most energy-dependent organ and requires tight regulation of blood flow to maintain energy supply, and therefore function.[32] Measurement of cerebral blood flow is vital not only for our understanding of cerebral hemodynamics, but also how blood flow impairment contributes to disease. Here, we present a non-invasive method to measure cerebral hemodynamics in real-time in the intact rat brain using transcranial CEU. We used the MCAO model of ischemic stroke in rats to demonstrate that CEU can detect physiological blood flow changes in the brain during ischemia and reperfusion. The decrease in cortical perfusion measured by CEU during MCAO (figures 3f and 6) is consistent with previous studies using well established techniques such as LDF (supplementary figure 8)[4, 33] and Laser Speckle Contrast Imaging.[34] While techniques like LDF are limited to sampling very small brain volumes and Laser Speckle only images the surface of the brain, CEU enabled us to longitudinally investigate how blood flow changed in different brain regions and across both hemispheres within each animal in response to ischemia and reperfusion. Our data highlight the complex and integrated response of the cerebral vasculature to ischemia where adjacent brain regions appear to have increased blood flow that may represent a physiological mechanism by which the cerebrovasculature attempts to rescue the ischemic region. Strikingly, we found a dramatic increase in perfusion following recanalization and reperfusion in a substantial proportion of the ipsilateral hemisphere. This is consistent with recent evidence of hyperperfusion in human ischemic stroke following endovascular thrombectomy.[35] In addition, we demonstrate the utility of transcranial CEU for the evaluation of brain region-specific vasomotion patterns and show that vasomotion is altered during ischemia and

reperfusion in the cortex. Therefore, transcranial CEU represents an advance in the non-invasive and real-time investigation of blood flow in the rodent brain and may reveal important physiological knowledge not currently possible by other imaging techniques.

Contrast enhanced ultrasound has been previously used to assess vascular perfusion in peripheral organs such as skeletal muscle, adipose tissue, kidney and heart in both animals and humans.[17, 19-22] Given the typical attenuating properties of bone on the ultrasound signal, previous studies had to perform a craniotomy to expose the brain in order to measure brain perfusion with CEU.[23, 24] Two human studies in ischemic stroke patients were able to use CEU to measure brain perfusion and showed a similar perfusion deficit with MCA stroke to perfusion-weighted MRI.[25, 26] While important, these studies were limited spatially (by the thickness of the human skull) to regions immediately behind the temple and temporally by the utilization of intravenous bolus injections of microbubbles to quantify blood flow dynamics. In the present study, the thinner rat skull compared to humans enabled penetration of the ultrasound signal through the skull, and a microbubble infusion allowed a steady state concentration of microbubbles in the circulation to be reached to allow accurate measurement of cerebral blood flow in the entire rat brain hemisphere before and after MCAO. The CEU method is relatively non-invasive, only requiring the insertion of a cannula into a vein such as the jugular, femoral or tail vein to enable constant infusion of microbubbles. By tracking the transit of microbubbles, CEU provides a measure of both flow velocity and blood volume to calculate an overall degree of tissue perfusion. Importantly, the microbubbles we use for CEU are approved for use in both animals and humans.[19, 21, 22, 36] Overall, transcranial CEU provides a platform for longitudinal and non-invasive assessment of cerebral

perfusion that will help uncover cerebrovascular responses in both physiological and pathophysiological states.

The tight regulation of cerebral blood flow is critical to maintain brain function.[32] This is not more clearly evident than following a stroke where patients can be left with long-lasting disabilities or even death due to irreversible damage to the brain.[37] The limited energy supply to one of the body's most energy-demanding organs leads to the degeneration of neurons, but the exact mechanisms by which damage occurs are still being elucidated.[38] The extent of blood flow changes that leads to ischemic damage in the brain requires accurate assessment of blood flow both during the ischemic period as well as upon reperfusion. Reperfusion therapy, either by pharmacological means with alteplase (recombinant tissue plasminogen activator) or surgical means with endovascular thrombectomy, is now the gold standard of ischemic stroke treatment.[39] Therefore, it is of vital importance to assess the extent of reperfusion within the brain following these treatments and whether they are associated with a positive outcome or otherwise.[5-7] In our hands, CEU assessment of cerebral hemodynamics showed a clear reduction in blood volume and velocity leading to decreased vascular perfusion in the ipsilateral cortex during MCAO and mirrors previous work using LDF (supplementary figure 8). Rather surprisingly, the extent of blood volume and vascular perfusion after filament withdrawal, as measured by CEU, was more than two-fold greater compared with baseline, suggesting the ischemic region was acutely and intensely hyperperfused upon blood flow restoration. This is at odds with LDF measurement of reperfusion which showed a restoration of flow but remained below baseline levels indicative of hypoperfusion. This difference could be due to the extent of tissue that is being assessed

as well as the method of capture of each technique. LDF is a point measurement with limited spatial information and depth of assessment into the tissue (a measurement volume of 0.012mm^3 in gray matter of the brain was calculated based on the parameters used in our experiments and models produced by Fredriksson et al.[40]). Also the response can be highly variable depending on the exact point of measurement used. LDF also relies on the Doppler shift of red blood cells as they pass under the probe and is proportional to both the velocity and number of red blood cells.[12] On the other hand, CEU detects the oscillation of microbubbles as they refill the circulation following high ultrasound destruction of microbubbles, and can assess the entire hemisphere of the brain (approximately 600mm^3)[41] with clear spatial information as to where changes in reperfusion are occurring. The advantage of CEU is that it provides an indicator of both flow and volume throughout the brain whereas LDF does not differentiate between the two. If the CEU flow velocity measurements are taken alone, these appear more akin to LDF measurements, i.e. during reperfusion, flow velocity is restored but not quite back to baseline levels, and it is blood volume (which is not definitively measured by LDF) that is substantially increased during reperfusion.

It is unclear from our studies whether this substantial hyperperfusion after MCAO is beneficial or detrimental to the brain. The brain's vascular response to ischemia would be to dilate vessels due to the reduction in perfusion pressure triggering the release of vasodilators,[42] which is an attempt to get as much oxygenated blood to the ischemic area as possible. This also occurs in other organs during ischemia such as the heart.[43] With this inherent dilation comes a substantial blood volume increase as reperfusion occurs, which is reflected in the CEU measurement. The provision of oxygen and glucose supply

to the previously ischemic brain through this hyperperfusion will undoubtedly allow the recovery of neurons affected by ischemia. However, it has been reported that hyperemia following stroke can actually result in low tissue oxygenation due to impaired capillary transit time heterogeneity,[44] along with the increased risk of oxidative injury during hyperperfusion post-stroke[45] and a dysfunction of neurovascular coupling.[13] This may represent an ischemia-reperfusion injury paradigm in the brain that has recently been proposed but not confirmed in human subjects due to the paucity of appropriate blood flow imaging techniques able to detect these changes.[6, 7] Interestingly, another study showed that hyperperfusion within 1 day post-MCAO was associated with smaller lesions but sustained hyperperfusion at 4 days post-MCAO was associated with infarct growth.[46] Further studies are required to delineate the benefit or harm of hyperperfusion, particularly in the current era where reperfusion therapy for stroke is the only current treatment option.

In addition to blood volume, flow velocity and vascular perfusion, transcranial CEU can also be used to measure vasomotion in the cerebrovasculature (figure 5). Vasomotion is the spontaneous and rhythmic oscillation of blood vessel tone that is proposed to be modulated by autoregulation and neurovascular coupling.[47, 48] Vasomotion has been observed in the human brain using near-infrared spectroscopy (NIRS) and transcranial Doppler,[47, 48] but both of these techniques are spatially limited to sampling only small, superficial regions of the brain. We have recently adapted CEU to assess and quantify vasomotion in skeletal muscle vasculature.[29] Here, we demonstrate that transcranial CEU can also be used to monitor and quantify region specific vasomotion in the cerebral vasculature. Our data show dampened vasomotion in the ipsilateral cortex during both

CCAO and MCAO and that vasomotion is substantially enhanced following reperfusion – a pattern that follows overall cerebral perfusion changes. While the changes during CCAO and MCAO may not be surprising given we have physically reduced blood flow by occluding a cerebral artery, the substantial rise in vasomotion at reperfusion may represent an alteration to normal autoregulatory and neurovascular coupling mechanisms to enable the overt increase in blood flow following ischemia. This conclusion is supported by a previous study where similar changes in vasomotion were observed using NIRS following acute ischemic stroke.[49]

In the current study, we assessed cerebral hemodynamics in both the ipsilateral (receiving MCAO) and contralateral (not receiving MCAO) hemispheres. While we did not observe any major alterations in perfusion within the contralateral cortex, we highlight a small, but sustained increase in vasomotion in the contralateral cortex during CCAO, MCAO and reperfusion. Intriguingly, we found that posterior sub-cortical blood volume in the contralateral hemisphere increased during the periods of CCAO and MCAO. This is reminiscent of the hemispheric vascular response shown in supplementary figure 7, and while the exact mechanisms for this are not clear from the present study, it is plausible that the entire cerebral vasculature (through autoregulatory and neurovascular coupling mechanisms) may be capable of responding to the ischemic event in the ipsilateral hemisphere by shunting more blood flow through the sub-cortical vessels in an attempt to restore ipsilateral perfusion.

In conclusion, transcranial CEU enables non-invasive tracking and quantification of cerebral hemodynamics in the rat brain that could be adapted for other species and disease models. We show that transcranial CEU can be readily applied to measure the

real-time quantification of cerebral blood flow in a rat model of stroke, demonstrating striking reductions during ischemia and hyperperfusion during vessel recanalization. While initially surprising, the identification of substantial post-stroke cerebral hyperperfusion using CEU indicates that the cerebral vasculature and its response in ischemia post-stroke warrants further interrogation.

Acknowledgements

None

Sources of funding

This work was supported by the University of Tasmania, Royal Hobart Hospital Research Foundation [18-206]; the National Health and Medical Research Council [APP1137776]; and the Rebecca L. Cooper Foundation [PG2018137].

Author Contribution Statement

DP and BAS conceived and designed the experiments. DP performed all contrast enhanced ultrasound imaging and subsequent analysis. BAS performed the middle cerebral artery occlusion to induce ischemic stroke. CJR performed some of the ultrasound analysis and contributed to generation of graphs and illustrations. SJB performed the vasomotion analysis. DWH and MAK assisted with the design of the experiments and interpretation of the results. DP and BAS wrote the manuscript and all named authors contributed to the editing of the manuscript.

Disclosures

The authors declare that there is no conflict of interest.

Supplementary Material

Supplementary material for this paper can be found at the journal website:

http://journals.sagepub.com/home/jcb

References

1. Astrup J, Siesjo BK, Symon L. Thresholds in cerebral ischemia - the ischemic penumbra. *Stroke* 1981; 12(6)**:** 723-5.
2. Balami JS, Sutherland BA, Edmunds LD, Grunwald IQ, Neuhaus AA, Hadley G *et al.* A systematic review and meta-analysis of randomized controlled trials of endovascular thrombectomy compared with best medical treatment for acute ischemic stroke. *Int J Stroke* 2015; 10(8)**:** 1168-78.
3. Nagel S, Papadakis M, Chen R, Hoyte LC, Brooks KJ, Gallichan D *et al.* Neuroprotection by dimethyloxalylglycine following permanent and transient focal cerebral ischemia in rats. *J Cereb Blood Flow Metab* 2011; 31(1)**:** 132-43.
4. Sutherland BA, Buchan AM. Alteplase treatment does not increase brain injury after mechanical middle cerebral artery occlusion in the rat. *J Cereb Blood Flow Metab* 2013; 33(11)**:** e1-7.
5. Sutherland BA, Neuhaus AA, Couch Y, Balami JS, DeLuca GC, Hadley G *et al.* The transient intraluminal filament middle cerebral artery occlusion model as a model of endovascular thrombectomy in stroke. *J Cereb Blood Flow Metab* 2016; 36(2)**:** 363-9.
6. Hsia AW, Luby M, Cullison K, Burton S, Armonda R, Liu A-H *et al.* Rapid Apparent Diffusion Coefficient Evolution After Early Revascularization: A Potential Marker of Secondary Injury? *Stroke* 2019**:** STROKEAHA. 119.025784.
7. Gauberti M, Lapergue B, Martinez de Lizarrondo S, Vivien D, Richard S, Bracard S *et al.* Ischemia-reperfusion injury after endovascular thrombectomy for ischemic stroke. *Stroke* 2018; 49(12)**:** 3071-3074.

8. Harston GW, Okell TW, Sheerin F, Schulz U, Mathieson P, Reckless I *et al.* Quantification of serial cerebral blood flow in acute stroke using arterial spin labeling. *Stroke* 2017; 48(1)**:** 123-130.

9. Fan AP, Jahanian H, Holdsworth SJ, Zaharchuk G. Comparison of cerebral blood flow measurement with [15O]-water positron emission tomography and arterial spin labeling magnetic resonance imaging: a systematic review. *Journal of Cerebral Blood Flow & Metabolism* 2016; 36(5)**:** 842-861.

10. Panerai RB, Jara JL, Saeed NP, Horsfield MA, Robinson TG. Dynamic cerebral autoregulation following acute ischaemic stroke: comparison of transcranial doppler and magnetic resonance imaging techniques. *Journal of Cerebral Blood Flow & Metabolism* 2016; 36(12)**:** 2194-2202.

11. Schramm P, Schellinger PD, Klotz E, Kallenberg K, Fiebach JB, Kulkens S *et al.* Comparison of perfusion computed tomography and computed tomography angiography source images with perfusion-weighted imaging and diffusion-weighted imaging in patients with acute stroke of less than 6 hours' duration. *Stroke* 2004; 35(7)**:** 1652-8.

12. Sutherland BA, Rabie T, Buchan AM. Laser Doppler flowmetry to measure changes in cerebral blood flow. *Methods Mol Biol* 2014; 1135**:** 237-48.

13. Sutherland BA, Fordsmann JC, Martin C, Neuhaus AA, Witgen BM, Piilgaard H *et al.* Multi-modal assessment of neurovascular coupling during cerebral ischaemia and reperfusion using remote middle cerebral artery occlusion. *J Cereb Blood Flow Metab* 2017; 37(7)**:** 2494-2508.

14. Tamura A, Graham D, McCulloch J, Teasdale G. Focal cerebral ischaemia in the rat: 2. Regional cerebral blood flow determined by [14C] iodoantipyrine autoradiography following middle cerebral artery occlusion. *Journal of Cerebral Blood Flow & Metabolism* 1981; 1(1)**:** 61-69.

15. Skarphedinsson J, Hårding H, Thoren P. Repeated measurements of cerebral blood flow in rats. Comparisons between the hydrogen clearance method and laser Doppler flowmetry. *Acta physiologica Scandinavica* 1988; 134(1)**:** 133-142.

16. Liao LD, Tsytsarev V, Delgado-Martinez I, Li ML, Erzurumlu R, Vipin A *et al.* Neurovascular coupling: in vivo optical techniques for functional brain imaging. *Biomed Eng Online* 2013; 12**:** 38.

17. Vincent MA, Dawson D, Clark AD, Lindner JR, Rattigan S, Clark MG *et al.* Skeletal muscle microvascular recruitment by physiological hyperinsulinemia precedes increases in total blood flow. *Diabetes* 2002; 51(1)**:** 42-8.

18. Hsu MJ, Esener SC, Eghtedari M, Hall DJ, Mattrey RF, Goodwin AP. Characterization of individual ultrasound microbubble dynamics with a light-scattering system. *Journal of biomedical optics* 2011; 16(6)**:** 067002.

19. Hu D, Remash D, Russell RD, Greenaway T, Rattigan S, Squibb KA *et al.* Impairments in Adipose Tissue Microcirculation in Type 2 Diabetes Mellitus Assessed by Real-Time Contrast-Enhanced Ultrasound. *Circ Cardiovasc Imaging* 2018; 11(4)**:** e007074.

20. Lindner JR. Molecular imaging of cardiovascular disease with contrast-enhanced ultrasonography. *Nat Rev Cardiol* 2009; 6(7)**:** 475-81.

21. Ng HLH, Premilovac D, Rattigan S, Richards SM, Muniyappa R, Quon MJ *et al.* Acute vascular and metabolic actions of the green tea polyphenol epigallocatechin 3-gallate in rat skeletal muscle. *J Nutr Biochem* 2017; 40**:** 23-31.

22. Russell RD, Hu D, Greenaway T, Blackwood SJ, Dwyer RM, Sharman JE *et al.* Skeletal Muscle Microvascular-Linked Improvements in Glycemic Control From Resistance Training in Individuals With Type 2 Diabetes. *Diabetes Care* 2017; 40(9)**:** 1256-1263.

23. Heppner P, Ellegala DB, Durieux M, Jane JA, Sr., Lindner JR. Contrast ultrasonographic assessment of cerebral perfusion in patients undergoing decompressive craniectomy for traumatic brain injury. *J Neurosurg* 2006; 104(5)**:** 738-45.

24. Rim SJ, Leong-Poi H, Lindner JR, Couture D, Ellegala D, Mason H *et al.* Quantification of cerebral perfusion with "Real-Time" contrast-enhanced ultrasound. *Circulation* 2001; 104(21)**:** 2582-7.

25. Bolognese M, Artemis D, Alonso A, Hennerici MG, Meairs S, Kern R. Real-time ultrasound perfusion imaging in acute stroke: assessment of cerebral perfusion deficits related to arterial recanalization. *Ultrasound Med Biol* 2013; 39(5)**:** 745-52.

26. Kern R, Diels A, Pettenpohl J, Kablau M, Brade J, Hennerici MG *et al.* Real-time ultrasound brain perfusion imaging with analysis of microbubble replenishment in acute MCA stroke. *J Cereb Blood Flow Metab* 2011; 31(8)**:** 1716-24.

27. Errico C, Osmanski BF, Pezet S, Couture O, Lenkei Z, Tanter M. Transcranial functional ultrasound imaging of the brain using microbubble-enhanced ultrasensitive Doppler. *Neuroimage* 2016; 124(Pt A)**:** 752-761.

28. Coggins M, Lindner J, Rattigan S, Jahn L, Fasy E, Kaul S *et al.* Physiologic hyperinsulinemia enhances human skeletal muscle perfusion by capillary recruitment. *Diabetes* 2001; 50(12)**:** 2682-90.

29. Blackwood SJ, Dwyer RM, Bradley EA, Keske MA, Richards SM, Rattigan S. Determination of skeletal muscle microvascular flowmotion with contrast-enhanced ultrasound. *Ultrasound in medicine & biology* 2017; 43(9)**:** 2013-2023.

30. Morlet J. Sampling theory and wave propagation. In: *Issues in acoustic Signal—image processing and recognition*. Springer, 1983, pp 233-261.

31. Torrence C, Compo GP. A practical guide to wavelet analysis. *Bulletin of the American Meteorological society* 1998; 79(1)**:** 61-78.

32. Attwell D, Buchan AM, Charpak S, Lauritzen M, Macvicar BA, Newman EA. Glial and neuronal control of brain blood flow. *Nature* 2010; 468(7321)**:** 232-43.

33. Taninishi H, Jung JY, Izutsu M, Wang Z, Sheng H, Warner DS. A blinded randomized assessment of laser Doppler flowmetry efficacy in standardizing outcome from intraluminal filament MCAO in the rat. *J Neurosci Methods* 2015; 241**:** 111-20.

34. Li Y, Zhu S, Yuan L, Lu H, Li H, Tong S. Predicting the ischemic infarct volume at the first minute after occlusion in rodent stroke model by laser speckle imaging of cerebral blood flow. *J Biomed Opt* 2013; 18(7)**:** 76024.

35. Shimonaga K, Matsushige T, Hosogai M, Hashimoto Y, Mizoue T, Ono C *et al.* Hyperperfusion after Endovascular Reperfusion Therapy for Acute Ischemic Stroke. *J Stroke Cerebrovasc Dis* 2019; 28(5)**:** 1212-1218.

36. Meneses AL, Nam MCY, Bailey TG, Magee R, Golledge J, Hellsten Y *et al.* Leg Blood Flow and Skeletal Muscle Microvascular Perfusion Responses to Submaximal Exercise in Peripheral Arterial Disease. *Am J Physiol Heart Circ Physiol* 2018.

37. Ganesh A, Luengo-Fernandez R, Wharton RM, Gutnikov SA, Silver LE, Mehta Z *et al.* Time Course of Evolution of Disability and Cause-Specific Mortality After Ischemic Stroke: Implications for Trial Design. *J Am Heart Assoc* 2017; 6(6).

38. Sutherland BA, Minnerup J, Balami JS, Arba F, Buchan AM, Kleinschnitz C. Neuroprotection for ischaemic stroke: Translation from the bench to the bedside. *Int J Stroke* 2012; 7(5)**:** 407-18.

39. Fischer U, Kaesmacher J, Mendes Pereira V, Chapot R, Siddiqui AH, Froehler MT *et al.* Direct Mechanical Thrombectomy Versus Combined Intravenous and Mechanical Thrombectomy in Large-Artery Anterior Circulation Stroke: A Topical Review. *Stroke* 2017; 48(10)**:** 2912-2918.

40. Fredriksson I, Larsson M, Stromberg T. Measurement depth and volume in laser Doppler flowmetry. *Microvasc Res* 2009; 78(1)**:** 4-13.

41. Sahin B, Aslan H, Unal B, Canan S, Bilgic S, Kaplan S *et al.* Brain volumes of the lamb, rat and bird do not show hemispheric asymmetry: a stereological study. *Image Analysis & Stereology* 2001; 20(1)**:** 9-13.

42. Powers WJ. Cerebral hemodynamics in ischemic cerebrovascular disease. *Ann Neurol* 1991; 29(3)**:** 231-40.

43. Gasser R, Brussee H, Wallner M, Kickenweiz E, Grisold M, Rotman B *et al.* Current views on mechanisms of vasodilation in response to ischemia and hypoxia. *Int J Angiol* 1993; 2(1)**:** 22-32.

44. Ostergaard L, Engedal TS, Moreton F, Hansen MB, Wardlaw JM, Dalkara T *et al.* Cerebral small vessel disease: Capillary pathways to stroke and cognitive decline. *J Cereb Blood Flow Metab* 2016; 36(2)**:** 302-25.

45. Sun MS, Jin H, Sun X, Huang S, Zhang FL, Guo ZN *et al.* Free Radical Damage in Ischemia-Reperfusion Injury: An Obstacle in Acute Ischemic Stroke after Revascularization Therapy. *Oxid Med Cell Longev* 2018; 2018**:** 3804979.

46. Wegener S, Artmann J, Luft AR, Buxton RB, Weller M, Wong EC. The time of maximum post-ischemic hyperperfusion indicates infarct growth following transient experimental ischemia. *PLoS One* 2013; 8(5)**:** e65322.

47. Schroeter ML, Bücheler MM, Preul C, Scheid R, Schmiedel O, Guthke T *et al.* Spontaneous slow hemodynamic oscillations are impaired in cerebral microangiopathy. *Journal of Cerebral Blood Flow & Metabolism* 2005; 25(12)**:** 1675-1684.

48. Giller CA, Hatab MR, Giller AM. Oscillations in cerebral blood flow detected with a transcranial Doppler index. *Journal of Cerebral Blood Flow & Metabolism* 1999; 19(4)**:** 452-459.

49. Phillip D, Schytz HW, Iversen HK, Selb J, Boas DA, Ashina M. Spontaneous low frequency oscillations in acute ischemic stroke: a near infrared spectroscopy (NIRS) study. *J. Neurol. Neurophysiol* 2014; 5(6)**:** 1000241.

Table 1 Cardiac and respiratory contribution to cortical vasomotion

Data expressed as percentage (%) of total vasomotion, mean ± SD. CONTRA = contralateral hemisphere, IPSI = ipsilateral hemisphere, CCAO = common carotid artery occlusion, MCAO = middle cerebral artery occlusion, RP = reperfusion. * indicates significant difference between CONTRA and IPSI hemispheres at a time point (*p < 0.05, **p < 0.01). # indicates significant increase from baseline in respiratory contribution during reperfusion (p<0.05).

	CONTRA				**IPSI**			
	Baseline	**CCAO**	**MCAO**	**RP**	**Baseline**	**CCAO**	**MCAO**	**RP**
Cardiac	57.5 ± 3.5	56.5 ± 3.7	56.8 ± 4.2	57.3 ± 3.7	58.3 ± 4.4	57.2 ± 3.8	55.8 ± 1.5	62.1 ± 2.4*
Respiratory	31.3 ± 0.4	30.5 ± 1.2	31.0 ± 0.3	29.7 ± 1.1	32.1 ± 2.1	32.1 ± 2.2*	33.1 ± 1.8**	28.1 ± 1.0*#

Figure Legends

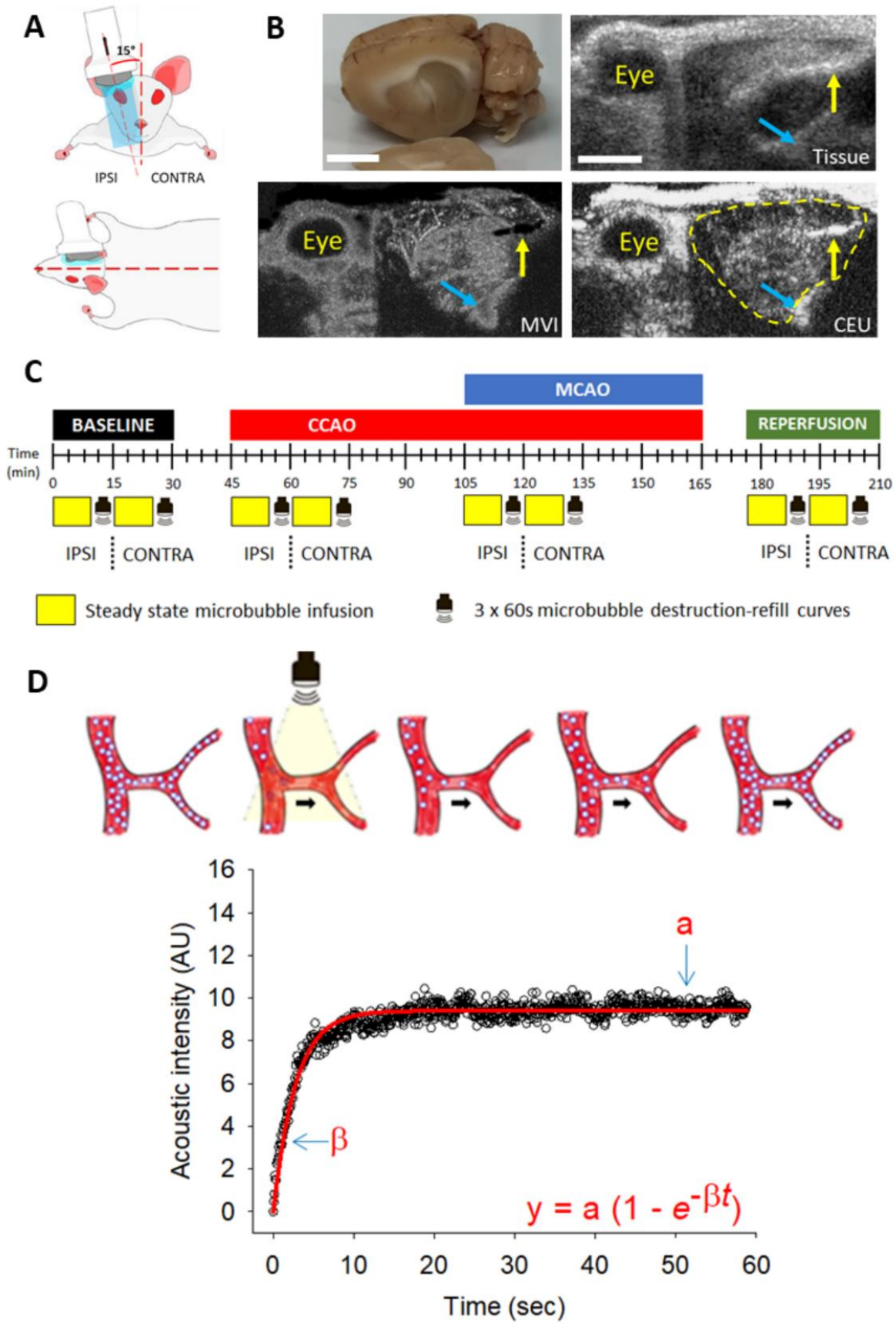
A
15°
IPSI
CONTRA
B
Eye
Tissue
Eye
MVI
Eye
CEU
C
MCAO
BASELINE
CCAO
REPERFUSION
Time (min)
0 15 30 45 60 75 90 105 120 135 150 165 180 195 210
IPSI CONTRA IPSI CONTRA IPSI CONTRA IPSI CONTRA
Steady state microbubble infusion
3 x 60s microbubble destruction-refill curves
D
Acoustic intensity (AU)
0 2 4 6 8 10 12 14 16
a
β
y = a (1 - e^-βt)
0 10 20 30 40 50 60
Time (sec)

Figure 1. Ultrasound imaging setup, experimental timeline and CEU quantification. (**A**) Schematic representation of ultrasound transducer placement and orientation above the animal's head on the ipsilateral (IPSI) side. The ultrasound transducer was positioned in line with the rat's eye and ear, tilted approximately 15° from the midline and fixed in place using a retort stand and clamp. Once imaging on the IPSI side was complete, the probe was moved to the contralateral (CONTRA) side and the same imaging repeated. (**B**) Clockwise from the top-left images are shown for; (i) excised rat brain with the corpus collosum (white matter tract) as the main visible structure delineating the cortex from sub-cortical regions; (ii) representative tissue ultrasound image of the rat's head with the corpus collosum visible within the brain; and representative images showing (iii) CEU imaging with the brain outlined by the yellow line and (iv) microvascular imaging (MVI). Yellow arrow = ear canal; cyan arrow = large artery at the base of the skull in each image. Scale bar = 0.5cm. (**C**) After anesthesia and vein cannulation, microbubbles were infused to steady-state over 9 minutes after which three 60 second destruction-refill curves were used to quantify changes in cerebral hemodynamics at the different time-points. CEU imaging was always performed first on the ipsilateral (IPSI – side receiving MCAO) followed by the contralateral (CONTRA) hemisphere of the brain at baseline, common carotid artery occlusion (CCAO), middle cerebral artery occlusion (MCAO) and reperfusion. (**D**) Diagrammatic representation of microbubble destruction-refill kinetics in the vasculature following a high mechanical index (1.20) burst of ultrasound (arrow indicates direction of blood flow). Reflow of microbubbles into the cerebrovasculature was assessed using low mechanical index (0.24), high frequency (15.2Hz) imaging over the course of 60 seconds. The resulting increase in acoustic intensity was plotted versus time

and fitted to an exponential increase to max equation (inset) where *y* = acoustic intensity at time *t*; the tangent to the acoustic intensity rise (β) represents flow velocity and the plateau of the curve (*a*) represents the blood volume. Vascular perfusion was calculated as the product of a x β.

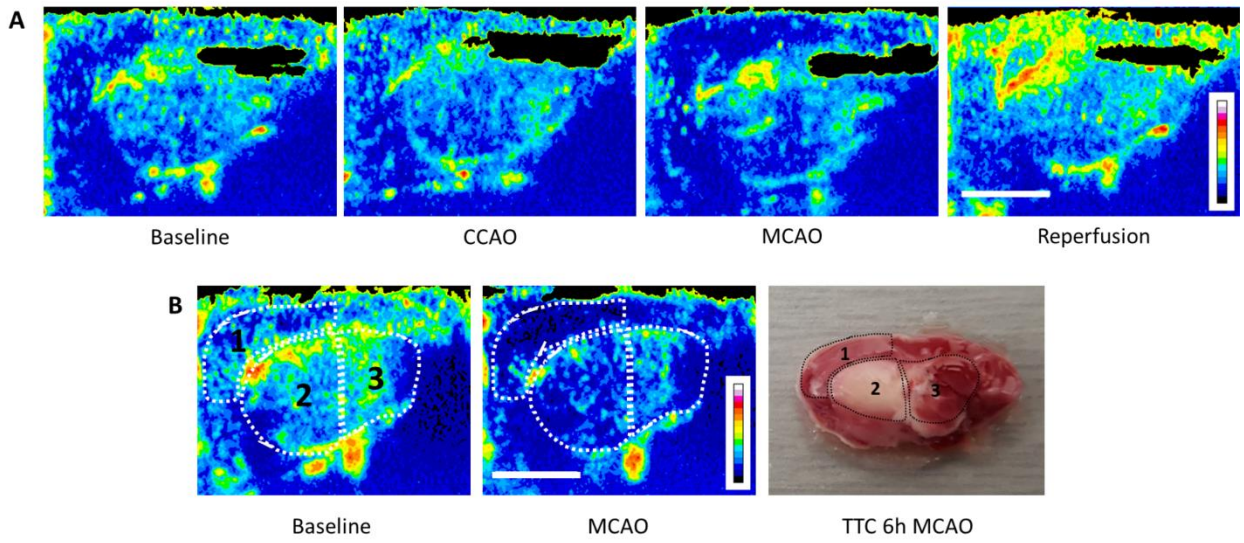

Figure 2. Spatial mapping of blood volume changes in the brain alongside histological changes following MCAO. (**A**) Blood volume maps demonstrating the acoustic intensity across the brain 60 seconds after microbubble destruction with high mechanical index ultrasound. Maps were generated from CEU images taken during baseline, CCAO, MCAO and reperfusion. During MCAO, a deficit in acoustic intensity can be clearly seen in the cortical (1) and striatal (2) regions of the brain that were then hyperperfused upon reperfusion (filament retraction). (**B**) A single rat underwent transcranial CEU prior to MCAO and blood volume maps were generated. The same rat was subjected to MCAO and transcranial CEU was repeated, with the blood volume map showing a substantial drop in the cortical (1) and striatal (2) regions, with less of a change in the posterior sub-cortical region (3). Scale bar = 0.5cm. The same rat continued to have MCAO for 6 hours before euthanasia. The brain was dissected, sectioned in the sagittal orientation, and stained with 2% TTC which stains viable tissue red/pink and injured tissue white. Both the cortex (1) and striatum (2) had some infarcted tissue, while the posterior sub-cortical region was mainly spared.

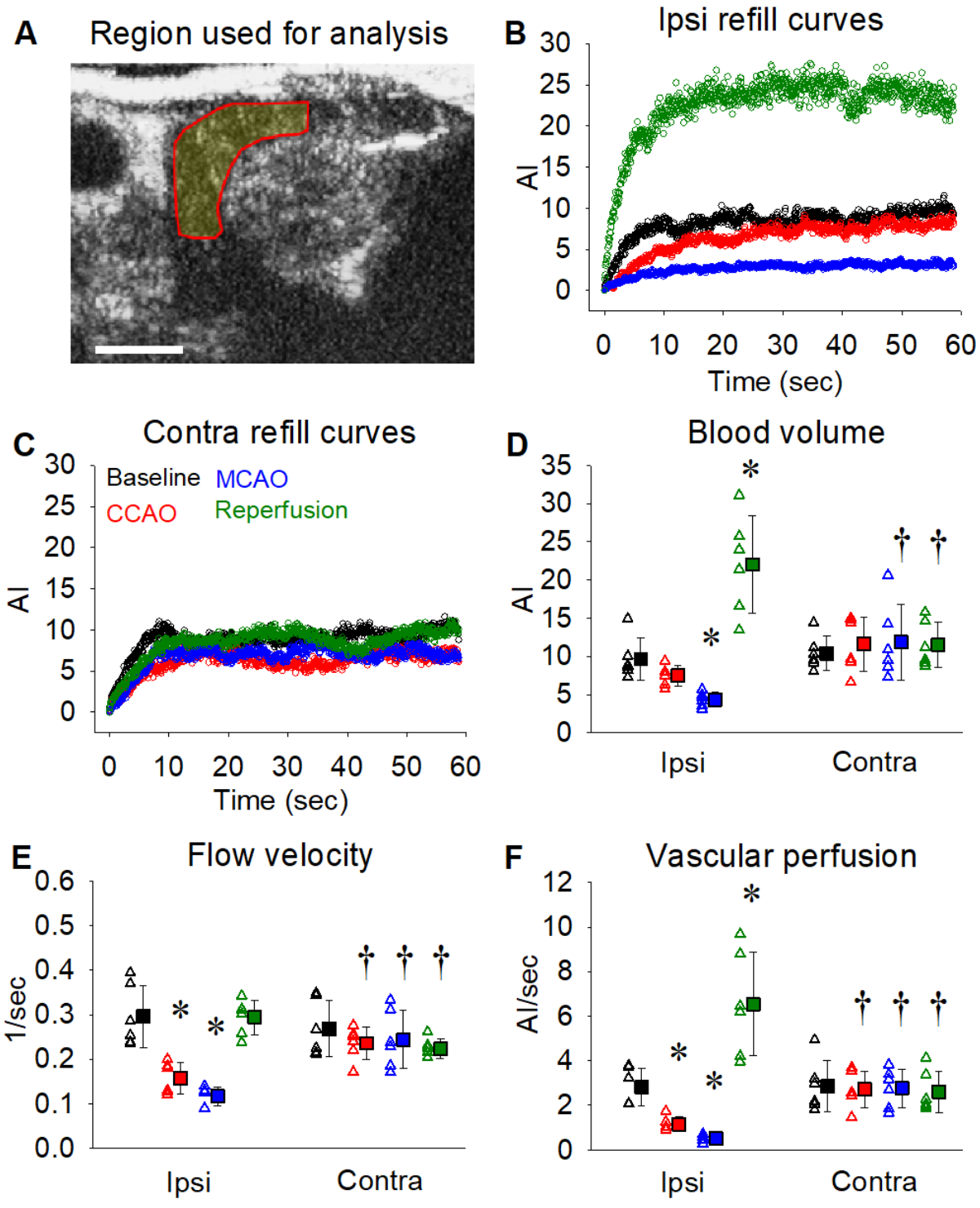

Figure 3. Cortical blood volume and vascular perfusion decrease markedly during MCAO and increase above baseline following reperfusion. The region of interest

used to quantify blood flow changes within the cortical region of each brain hemisphere is illustrated in panel (**A**). Representative 60 second destruction-refill curves from one animal for each of the time-points (baseline, CCAO, MCAO and reperfusion) are shown for the ipsilateral (**B**) and contralateral (**C**) cortical regions. Blood volume (**D**), flow velocity (**E**) and vascular perfusion (**F**) were calculated for each time-point across both ipsilateral and contralateral cortical regions as outlined in figure 1d. Open triangles represent individual values from independent experiments and filled squares represent the means ± SD for 6 rats. Where error bars are not visible, they are within the symbol. * denotes $p<0.05$ vs within group baseline, † denotes $p<0.05$ vs ipsilateral at the same time-point as assessed by repeated measures two-way ANOVA with SNK post-hoc. Scale bar = 0.5cm.

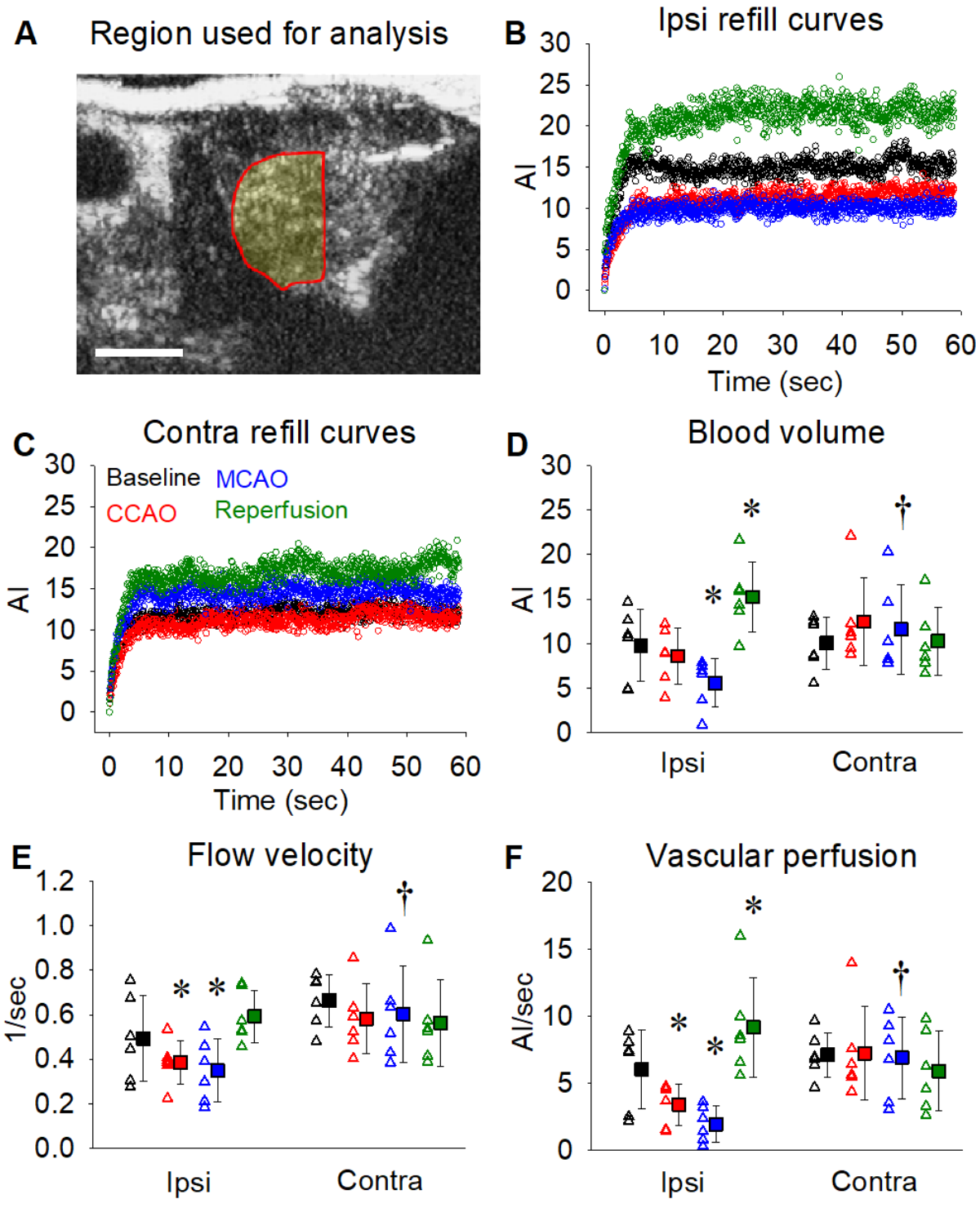

Figure 4. Striatal blood volume and vascular perfusion decrease markedly during MCAO and increase above baseline following reperfusion. The region of interest

used to quantify blood flow changes within the striatal region of each brain hemisphere is illustrated in panel (**A**). Representative 60 second destruction-refill curves from one animal for each of the time-points (baseline, CCAO, MCAO and reperfusion) are shown for the ipsilateral (**B**) and contralateral (**C**) striatal regions. Blood volume (**D**), flow velocity (**E**) and vascular perfusion (**F**) were calculated for each time-point across both ipsilateral and contralateral striatal regions as outlined in figure 1d. Open triangles represent individual values from independent experiments and filled squares represent the means ± SD for 6 rats. * denotes $p<0.05$ vs within group baseline, † denotes $p<0.05$ vs ipsilateral at the same time-point as assessed by repeated measures two-way ANOVA with SNK post-hoc. Scale bar = 0.5cm.

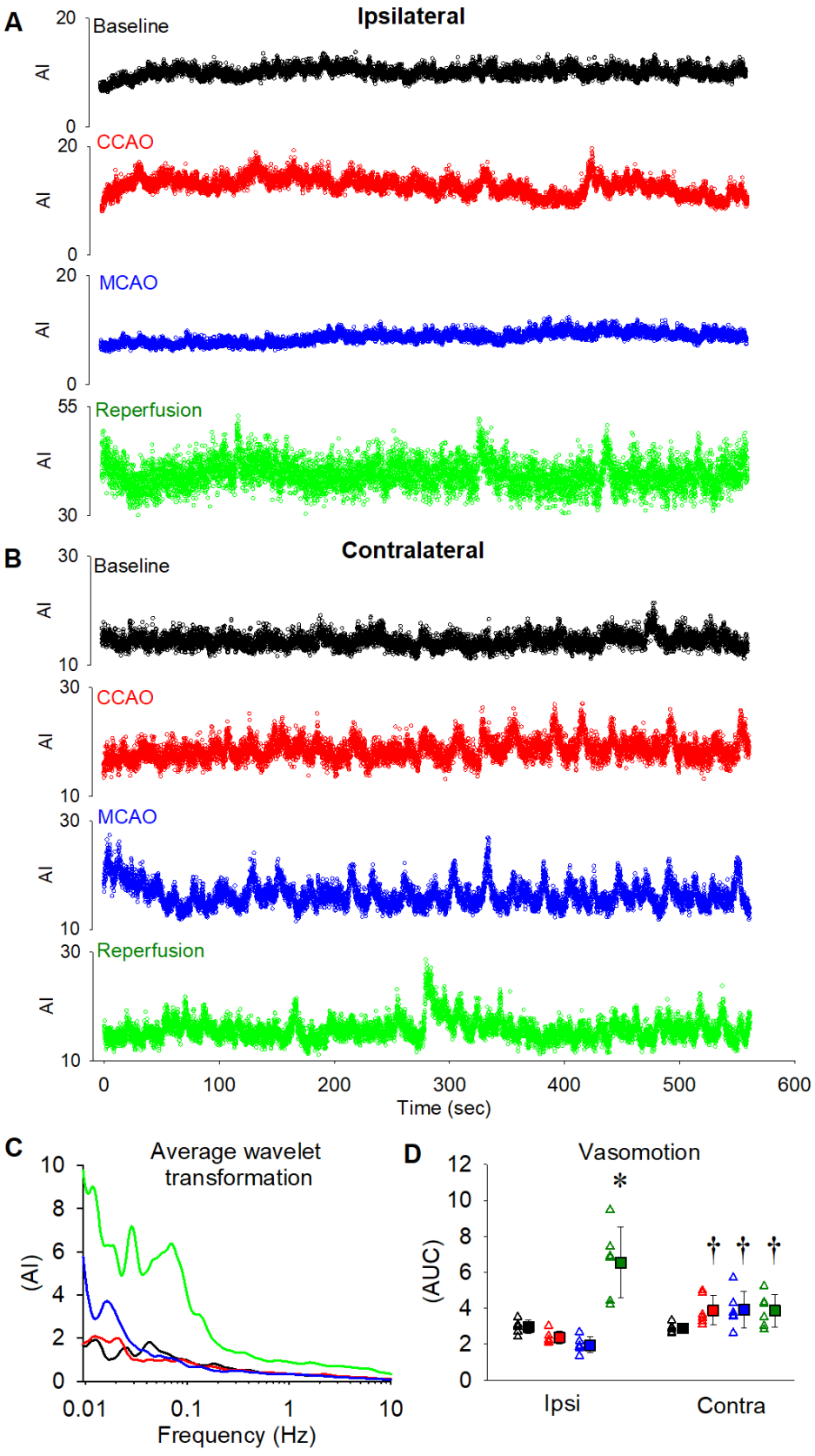
A
Ipsilateral
Baseline
CCAO
MCAO
Reperfusion
AI
20
0
55
30
B
Contralateral
30
10
0
100
200
300
400
500
600
Time (sec)
C
Average wavelet transformation
(AI)
Frequency (Hz)
0.01
0.1
1
10
D
Vasomotion
(AUC)
12
Ipsi
Contra

Figure 5. Assessment of cortical vasomotion on both the ipsilateral (MCAO) and contralateral (no MCAO) hemispheres. A 9-minute infusion was used to ensure steady-state microbubble concentrations prior to assessment of cerebral hemodynamics. Representative 9-minute traces from a single experiment are shown from the ipsilateral cortex (**A**) and contralateral cortex (**B**) for baseline (black), CCAO (red), MCAO (blue) and reperfusion (green). Spectral analysis was performed on these data and a representative frequency distribution is shown for the ipsilateral cortex (**C**). Total vasomotion patterns were assessed for each experiment and the quantified data are shown in panel **D**. Open triangles represent individual values from independent experiments and filled squares represent the means ± SD for 6 rats. Where error bars are not visible, they are within the symbol. * denotes $p<0.05$ vs within group baseline, † denotes $p<0.05$ vs ipsilateral at the same time-point as assessed by repeated measures two-way ANOVA with SNK post-hoc.

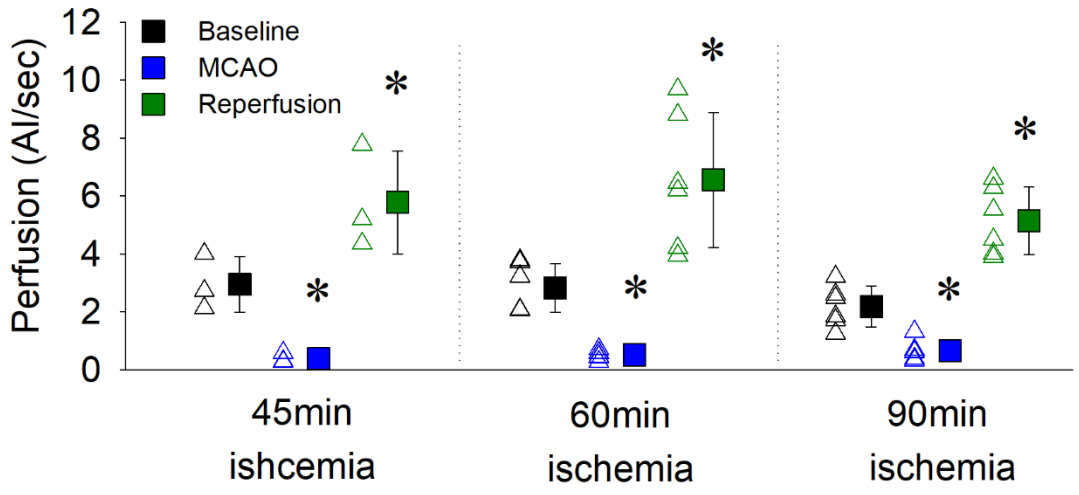

Figure 6. Cortical vascular perfusion increased above baseline following reperfusion irrespective of MCAO duration. Rats underwent MCAO for either 45, 60 or 90 minutes, with a significant reduction in vascular perfusion detected in the cortex. Once reperfusion occurred, hyperperfusion in the cortex was observed following all durations of MCAO. Open triangles represent individual values from independent experiments and filled squares represent the means ± SD for 3-6 rats. Where error bars are not visible, they are within the symbol. * denotes $p<0.05$ vs within group baseline as assessed by repeated measures two-way ANOVA with SNK post-hoc.